

## *Supporting Information*

### **Structure and Assembly Studies of Two Planar Dy(III) Single Molecule Magnets with Double Relaxation**

Shui Yu,<sup>a,b,‡</sup> Lan Liu,<sup>a,‡</sup> Limin Zhou,<sup>a</sup> Dongcheng Liu,<sup>\*,a</sup> Chuying Chen,<sup>a</sup> Hua-Hong Zou,<sup>a</sup> Huancheng Hu,<sup>\*,a</sup> Yuning Liang,<sup>a</sup> Fupei Liang,<sup>a</sup> Zilu Chen<sup>\*,a</sup>

<sup>a</sup>State Key Laboratory for Chemistry and Molecular Engineering of Medicinal Resources, School of Chemistry and Pharmaceutical Sciences, Guangxi Normal University, Guilin 541004, P. R. China. E-mail: ldcheng@mailbox.gxnu.edu.cn, siniantongnian@126.com, zlchen@mailbox.gxnu.edu.cn

<sup>b</sup>School of Pharmacy, Binzhou Medical University, Yantai 264003, P. R. China.

‡These authors contributed equally to this work.

## **1. Experimental**

### **Materials and Measurements.**

All chemical reagents were used as commercially received without further purification.

The Fourier transform infrared (FT-IR) data of the two complexes were collected on

Perkin-Elmer Spectrum One FT-IR spectrometer using the corresponding KBr Pellets

in the wavenumber range of 4000-400 cm<sup>-1</sup>. The powder X-ray diffraction (PXRD)

measurements were carried out on a Rigaku D/max 2500v/pc diffractometer equipped

with Cu-K $\alpha$  radiation ( $\lambda = 1.5418 \text{ \AA}$ ) at 40 kV and 40 mA, with a step size of 0.02° in

2θ and a scan speed of 5° min<sup>-1</sup>. Elemental analyses for C, H, and N for the two

complexes were performed on an Elementar Micro cube C, H, N elemental analyzer.

The TG analyses (30-1000 °C) for **1** and **2** were conducted on a PerkinElmer Diamond

TG/DTA thermal analyzer in a flowing nitrogen atmosphere with a heating rate of 5 °C

min<sup>-1</sup>. All magnetic data were measured on a Quantum Design MPMS SQUID-XL-7

SQUID magnetometer furnished with a 7 T magnet. The magnetic data of the two

complexes were corrected with a consideration of diamagnetic contribution from the

sample and the sample holder.

### **Single-crystal X-ray crystallography.**

Diffraction data for these complexes were collected on a Bruker SMART CCD

diffractometer (Mo K $\alpha$  radiation and  $\lambda = 0.71073 \text{ \AA}$ ) in  $\Phi$  and  $\omega$  scan modes. The

structures were solved by direct methods, followed by difference Fourier syntheses, and

then refined by full-matrix least-squares techniques on F<sup>2</sup> using SHELXL. All other

non-hydrogen atoms were refined with anisotropic thermal parameters. Hydrogen

atoms were placed at calculated positions and isotropically refined using a riding model.

The lattice molecules in **2** couldn't be modelled directly probably due to heavy disorder.

The use of SQUEEZE procedure gave a volume of 1070 Å with 156 electrons in one unit cell, which corresponds to four MeOH, two CH<sub>3</sub>CN and four H<sub>2</sub>O molecules. Table S3 summarizes X-ray crystallographic data and refinement details for the complexes. Full details can be found in the CIF files provided in the Supporting Information. The CCDC reference numbers are 2291880 and 2291881 for **1** and **2**, respectively.

#### **The detection method for intermediates:**

The similar methods and procedures were used to test and track the assembly process for complexes **1** and **2**. Therefore, only that for **1** was presented here in detail as an example. The synthesis of complex **1** was carried out using solvothermal method in sealed. 20 parallel reactions were carried out simultaneously in an oven at 80 °C with all required raw materials sealed in high-temperature resistant Pyrex tubes. When the reaction time reached 5, 15, 25, 40, 60, 90, 130, 180, 240, and 360 minutes, glass tubes were taken out successively, from which 0.2 ml of reaction solution was quickly taken out, diluted with 20 mL of methanol, and then subjected to HR-ESI tests.

#### **ESI-MS measurement.**

ESI-MS measurements were conducted at a capillary temperature of 275 °C. Aliquots of the solution were injected into the device at 0.3 mL/h. The mass spectrometer used for the measurements was a Thermo Exactive, and the data were collected in positive and negative ion modes. The spectrometer was previously calibrated with the standard tune mix to give a precision of ca. 2 ppm within the region of 200 - 2000 m/z. The capillary voltage was 50 V, the tube lens voltage was 150 V,

and the skimmer voltage was 25 V. The in-source energy was set within the range of 0-80 eV with a gas flow rate at 10% of the maximum.

## 2. characterization

The TG analyses of **1** and **2** are shown in Fig. S5 and S6, respectively. Upon increasing the temperature, **1** underwent a fast weight loss of 6.67% before 80 °C with a subsequent much slower weight loss, which corresponds to the loss of five acetonitrile, (calcd 6.62%) per formular unit of **1**. The followed was a subsequent much slower weight loss at 80 - 347 °C, which corresponds to the loss of the ligands of L'. The followed weight losses were due to the collapse of the Schiff base ligands in **1**, which didn't come to an end even when the temperature reaches 1000 °C. Upon heating, a continuous weight loss was found. It underwent a fast weight loss before 75 °C with a subsequent slower weight loss. The weight loss of 7.24% before 182 °C is due to the loss of free solvent molecules (four H<sub>2</sub>O, four CH<sub>3</sub>OH and two CH<sub>3</sub>CN) per formular unit (calcd 8.45%). Then it keep stable at 182 - 230 °C. Upon heating, the weight losses were due to loss of coordinated Cl and skeleton collapse. The followed weight loss was incomplete even upon being heated at 1000 °C. The purities of the collected bulky crystalline samples of complexes **1** and **2** were confirmed by the nice agreement of the experimental PXRD curves with the simulated ones derived from the corresponding single crystal X-ray diffraction data as shown in Fig. S3 and S4, respectively.

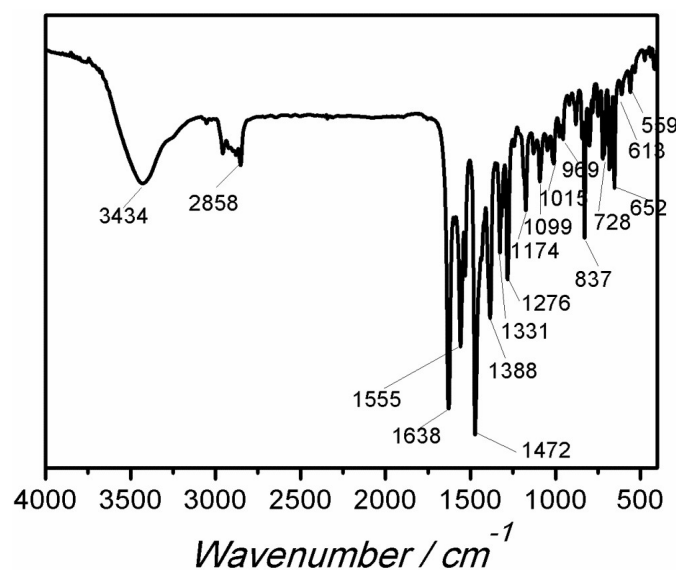


Fig. S1 FT-IR spectrum of 1.

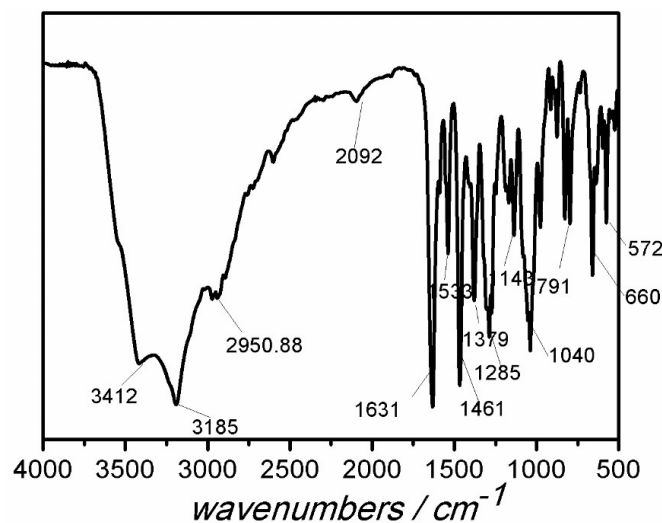


Fig. S2 FT-IR spectrum of 2.

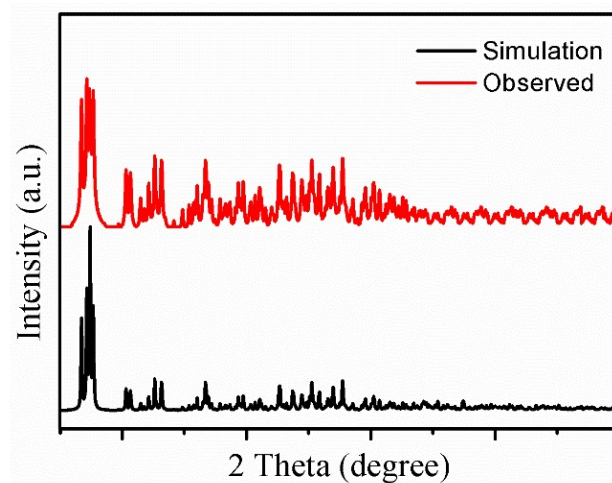
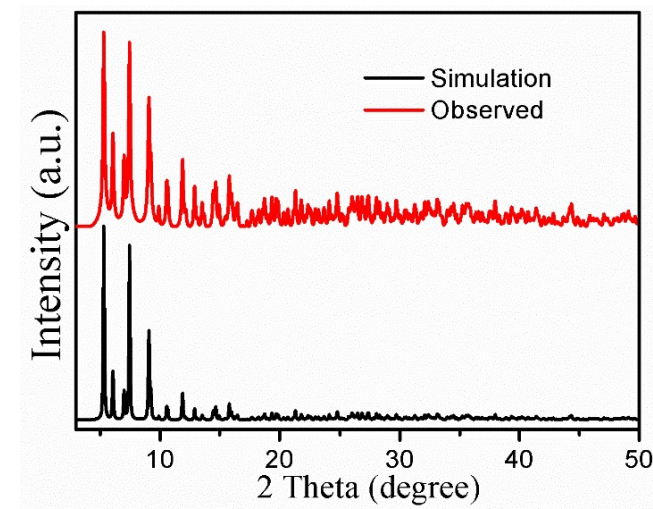
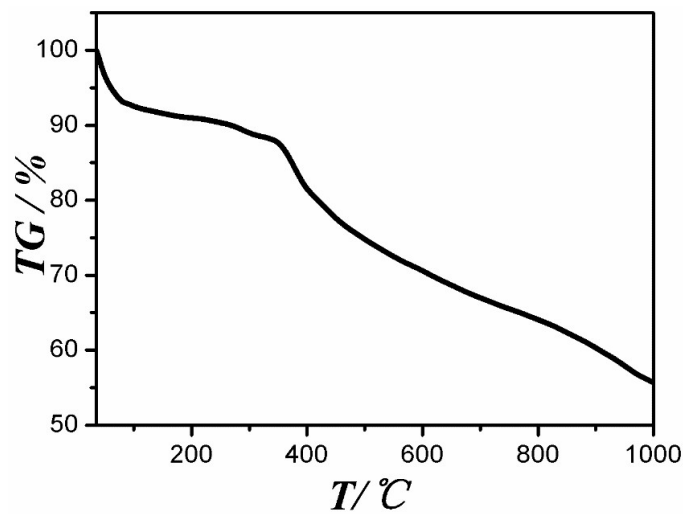


Fig. S3 PXRD patterns of 1.



**Fig. S4** PXRD patterns of 2.



**Fig. S5** TG of 1.

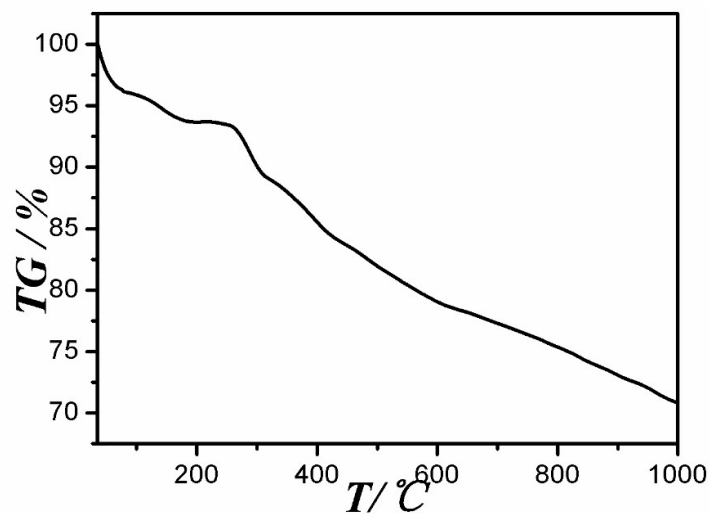


**Fig. S6** TG of 2.

**Table S1.** Crystallographic data of **1** and **2**.

Compound	<b>1</b>	<b>2</b>
Formula	C <sub>96</sub> H <sub>89</sub> Br <sub>10</sub> Dy <sub>4</sub> N <sub>13</sub> O <sub>14</sub>	C <sub>78</sub> H <sub>116</sub> Br <sub>6</sub> Cl <sub>4</sub> Dy <sub>6</sub> N <sub>8</sub> O <sub>36</sub>
fw	3097.90	3338.00
T / K	100(2)	100(2)
$\lambda$ / Å	0.71073	1.54184
crystal system	Triclinic	Triclinic
space group	<i>P</i> 	<i>P</i> 
<i>a</i> / Å	14.4150 (2)	11.8746 (4)
<i>b</i> / Å	14.6798 (3)	15.0586 (6)
<i>c</i> / Å	15.0212 (2)	17.1270 (6)
$\alpha$ / °	108.858 (2)	75.517 (3)
$\beta$ / °	103.154 (1)	88.043 (3)
$\gamma$ / °	110.262 (2)	86.203 (3)
<i>V</i> / Å <sup>3</sup>	2607.36 (9)	2958.24 (19)
Z	1	1
D <sub>c</sub> / g·cm <sup>-3</sup>	1.973	1.715
$\mu$ / mm <sup>-1</sup>	6.73	23.59
2θ / °	3.200 to 49.000	5.200 to 157.600
<i>F</i> (000)	1482	1446.0
reflns collected	11732	34598
reflns unique	8981	18744
<i>R</i> <sub>int</sub>	0.050	0.081
GOF on <i>F</i> <sup>2</sup>	1.086	1.051
<i>R</i> <sub>1</sub> (I > 2σ(I))	0.0423	0.0670
$\omega R_2$ (I > 2σ(I))	0.1045	0.1799
<i>R</i> <sub>1</sub> (all data)	0.0627	0.0727
$\omega R_2$ (all data)	0.1112	0.1844

**Table S2.** Selected bond lengths / Å and bond angles / ° for **1**.

Dy1-O1	2.326 (4)	Dy2-O1	2.364 (3)	O1-Dy1-O3	69.25 (12)
Dy1-O2	2.321 (4)	Dy2-O1A	2.362 (3)	O1-Dy1-N1	72.97 (14)
Dy1-O3	2.340 (4)	Dy2-O2A	2.538 (4)	O1-Dy1-N2	109.67 (15)
Dy1-N1	2.526 (5)	Dy2-O3	2.503 (4)	O1-Dy1-O5	146.43 (14)
Dy1-N2	2.519 (5)	Dy2-N3	2.474 (5)	O1-Dy1-O6A	69.61 (12)
Dy1-O4	2.240 (4)	Dy2-N4	2.522 (5)	O2-Dy1-O1	78.71 (13)
Dy1-O5	2.413 (5)	Dy2-O6	2.392 (4)	O2-Dy1-O3	142.61 (13)
Dy1-O6A	2.487 (4)	Dy2-O7	2.212 (4)	O2-Dy1-N1	73.54 (14)
O3-Dy1-N1	112.97 (14)	N2-Dy1-N1	69.66 (16)	O2-Dy1-N2	137.23 (14)
O3-Dy1-N2	73.91 (14)	O4-Dy1-O1	141.17 (14)	O2-Dy1-O5	74.37 (15)
O3-Dy1-O5	142.04 (15)	O4-Dy1-O2	119.38 (15)	O2-Dy1-O6A	65.99 (12)
O3-Dy1-O6A	84.69 (12)	O4-Dy1-O3	78.94 (15)	O6A-Dy1-N1	128.84 (14)
O5-Dy1-N1	80.40 (17)	O4-Dy1-N1	142.52 (15)	O6A-Dy1-N2	156.78 (14)
O5-Dy1-N2	78.67 (17)	O4-Dy1-N2	80.99 (17)	O1A-Dy2-O1	72.58 (13)
O5-Dy1-O6A	115.35 (15)	O4-Dy1-O5	71.18 (16)	O1A-Dy2-O2A	73.85 (12)
O3-Dy2-O2A	160.87 (12)	O4-Dy1-O6A	86.21 (14)	O1-Dy2-O2A	132.03 (12)
O3-Dy2-N4	90.72 (14)	O1A-Dy2-O6	70.69 (12)	O1A-Dy2-O3	111.88 (12)
N3-Dy2-O2A	105.78 (14)	O1-Dy2-O6	72.90 (12)	O1-Dy2-O3	65.95 (12)
N3-Dy2-O3	81.25 (14)	O6-Dy2-O2A	64.18 (12)	O1-Dy2-N3	81.71 (13)
N3-Dy2-N4	73.34 (14)	O6-Dy2-O3	134.80 (12)	O1A-Dy2-N3	141.75 (13)
O7-Dy2-O1	121.93 (13)	O6-Dy2-N3	75.00 (13)	O1A-Dy2-N4	138.55 (13)
O7-Dy2-O1A	74.45 (12)	O6-Dy2-N4	117.51 (15)	O1-Dy2-N4	148.27 (14)
O7-Dy2-O2A	79.46 (13)	O7-Dy2-N3	143.78 (13)	O7-Dy2-N4	73.71 (14)
O7-Dy2-O3	84.54 (13)	O7-Dy2-O6	134.96 (13)	O26-Dy2-O8	80.4 (4)

**Table S3.** Selected bond lengths / Å and bond angles / ° for 2.

Dy1-O1	2.293 (5)	Dy2-O1	2.394 (6)	Dy3-O1	2.465 (5)
Dy1-O2	2.448 (5)	Dy2-O2	2.368 (5)	Dy3-O2	2.366 (5)
Dy1-O3	2.385 (6)	Dy2-O3	2.603 (5)	Dy3-O6	2.222 (6)
Dy1-O3A	2.338 (6)	Dy2-O5A	2.338 (6)	Dy3-O10	2.459 (6)
Dy1-N1	2.460 (7)	Dy2-O6	2.336 (6)	Dy3-O11	2.423 (6)
Dy1-O5	2.308 (5)	Dy2-O7	2.400 (6)	Dy3-N3	2.490 (8)
Dy1-O13	2.397 (6)	Dy2-N2	2.479 (7)	Dy3-O13	2.287 (6)
Dy1-O14	2.405 (6)	Dy2-O9	2.237 (6)	Dy3-Cl1	2.692 (2)
O1-Dy1-O2	61.79 (18)	O3A-Dy1-O2	127.73 (18)	O5-Dy1-O2	140.11 (19)
O1-Dy1-O3	83.20 (19)	O3-Dy1-O2	66.44 (18)	O5-Dy1-O3A	74.3 (2)
O1-Dy1-O3A	83.71 (19)	O3A-Dy1-O3	71.9 (2)	O5-Dy1-O3	97.86 (19)
O1-Dy1-N1	130.7 (2)	O3-Dy1-N1	70.5 (2)	O5-Dy1-N1	70.6 (2)
O1-Dy1-O5	156.33 (19)	O3A-Dy1-N1	123.2 (2)	O5-Dy1-O13	116.3 (2)
O1-Dy1-O13	76.5 (2)	O3A-Dy1-O13	142.2 (2)	O5-Dy1-O14	72.2 (2)
O1-Dy1-O14	94.4 (2)	O3-Dy1-O13	135.48 (19)	O13-Dy1-O2	69.04 (18)
O2-Dy1-N1	69.5 (2)	O3-Dy1-O14	148.1 (2)	O13-Dy1-N1	93.8 (2)
O14-Dy1-O2	139.17 (19)	O3A-Dy1-O14	76.3 (2)	O13-Dy1-O14	73.5 (2)
O14-Dy1-N1	129.5 (2)	O1-Dy2-O3	76.75 (17)	O1-Dy2-O7	78.32 (19)
O2-Dy2-O1	61.60 (19)	O5A-Dy2-O1	92.24 (19)	O1-Dy2-N2	134.0 (2)
O2-Dy2-O3	64.19 (17)	O5A-Dy2-O2	130.11 (19)	O5A-Dy2-O7	74.4 (2)
O2-Dy2-O7	131.1 (2)	O5A-Dy2-O3	68.97 (19)	O5A-Dy2-N2	106.2 (2)
O2-Dy2-N2	122.8 (2)	O6-Dy2-O7	74.3 (2)	O7-Dy2-O3	134.24 (18)
O6-Dy2-O1	76.82 (19)	O6-Dy2-N2	65.3 (2)	N2-Dy2-O3	149.2 (2)
O6-Dy2-O2	70.47 (19)	O9-Dy2-O1	154.04 (19)	O9-Dy2-O7	122.5 (2)
O6-Dy2-O3	134.24 (19)	O9-Dy2-O2	104.6 (2)	O9-Dy2-N2	71.8 (2)
O6-Dy2-O5A	148.3 (2)	O9-Dy2-O3	77.37 (19)	O1-Dy3-N3	115.2 (2)
O2-Dy3-O1	60.58 (18)	O9-Dy2-O5A	80.4 (2)	O1-Dy3-Cl1	141.97 (13)
O2-Dy3-O10	143.9 (2)	O9-Dy2-O6	121.3 (2)	O10-Dy3-O1	136.5 (2)
O2-Dy3-O11	131.9 (2)	O6-Dy3-O1	77.5 (2)	O10-Dy3-N3	66.0 (2)
O2-Dy3-N3	144.6 (2)	O6-Dy3-O2	72.45 (19)	O10-Dy3-Cl1	78.93 (16)
O2-Dy3-Cl1	82.39 (14)	O6-Dy3-O10	81.0 (2)	O11-Dy3-O1	72.6 (2)
O13-Dy3-O1	75.3 (2)	O6-Dy3-O11	88.0 (2)	O11-Dy3-O10	69.3 (2)
O13-Dy3-O2	72.33 (19)	O6-Dy3-N3	143.0 (2)	O11-Dy3-N3	65.6 (2)
O13-Dy3-O10	135.9 (2)	O6-Dy3-O13	142.8 (2)	O11-Dy3-Cl1	145.36 (16)
O13-Dy3-O11	107.1 (2)	O6-Dy3-Cl1	100.65 (17)	N3-Dy3-Cl1	89.37 (19)
O13-Dy3-N3	72.8 (2)	O13-Dy3-Cl1	86.06 (16)		

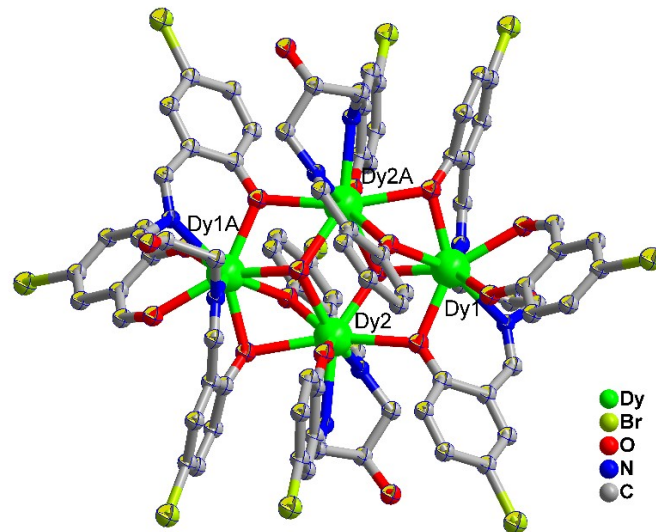


**Fig. S7** The structure of **1** with 30% probability ellipsoid and selected atoms labelled.

Hydrogen atoms are omitted for clarity. Symmetry code: A)  $-x + 1, -y + 1, -Z + 1$ .

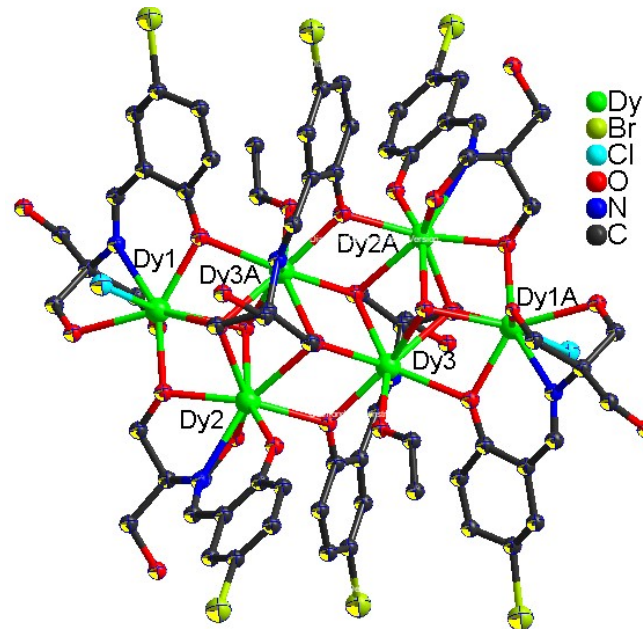


**Fig. S8** The structure of **2** with 30% probability ellipsoid and selected atoms labelled.

Hydrogen atoms are omitted for clarity. Symmetry code: A)  $-x + 1, -y + 1, -Z + 1$ .

**Table S4.** SHAPE analysis of Dy1 and Dy2 in **1**

Configuration	ABOXIY(Dy1)	ABOXIY(Dy2)
Octagon ( $D_{8h}$ )	29.832	30.059
Heptagonal pyramid ( $C_{7v}$ )	21.038	22.189
Hexagonal bipyramid ( $D_{6h}$ )	15.226	14.981
Cube ( $O_h$ )	8.282	8.848
<b>Square antiprism (<math>D_{4d}</math>)</b>	<b>0.829</b>	<b>1.173</b>
Triangular dodecahedron ( $D_{2d}$ )	2.582	2.884
Johnson gyrobifastigium J26 ( $D_{2d}$ )	15.593	14.951
Johnson elongated triangular bipyramid J14 ( $D_{3h}$ )	26.498	27.063
Biaugmented trigonal prism J50 ( $C_{2v}$ )	3.222	3.205
Biaugmented trigonal prism ( $C_{2v}$ )	2.656	2.629
Snub diphenoïd J84 ( $D_{2d}$ )	5.328	5.555
Triakis tetrahedron ( $T_d$ )	8.722	9.520
Elongated trigonal bipyramid ( $D_{3h}$ )	23.403	23.756

**Table S5.** SHAPE analysis of Dy1, Dy2 and Dy3 in **2**

Configuration	ABOXIY(Dy1)	Dy2	Dy3
Octagon ( $D_{8h}$ )	28.969	28.677	31.584
Heptagonal pyramid ( $C_{7v}$ )	23.494	20.055	20.249
Hexagonal bipyramid ( $D_{6h}$ )	15.748	12.228	15.923
Cube ( $O_h$ )	11.819	11.574	12.388
Square antiprism ( $D_{4d}$ )	2.445	4.580	3.690
Triangular dodecahedron ( $D_{2d}$ )	2.477	4.085	2.371
Johnson gyrobifastigium J26 ( $D_{2d}$ )	13.687	8.422	12.202
Johnson elongated triangular bipyramid J14 ( $D_{3h}$ )	28.202	24.262	25.646
Biaugmented trigonal prism J50 ( $C_{2v}$ )	2.777	3.731	2.741
<b>Biaugmented trigonal prism (<math>C_{2v}</math>)</b>	<b>2.067</b>	<b>3.482</b>	<b>1.863</b>
Snub diphenoïd J84 ( $D_{2d}$ )	4.233	5.781	4.062
Triakis tetrahedron ( $T_d$ )	12.266	12.203	12.769
Elongated trigonal bipyramid ( $D_{3h}$ )	24.183	19.895	22.526

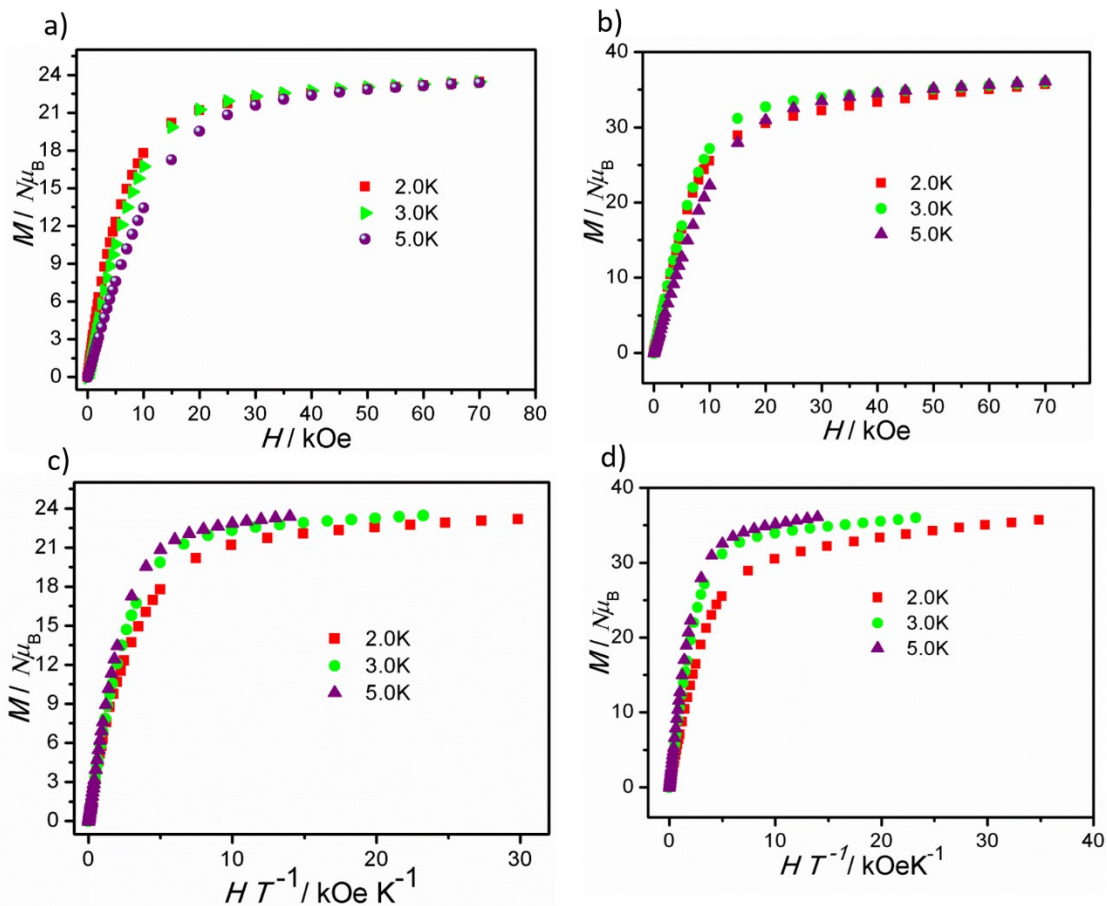


**Fig. S9** Plots of  $M$  vs.  $H$  and  $H T^{-1}$  for **1** (a and c) and **2** (b and d) measured at 2.0, 3.0 and 5.0 K.

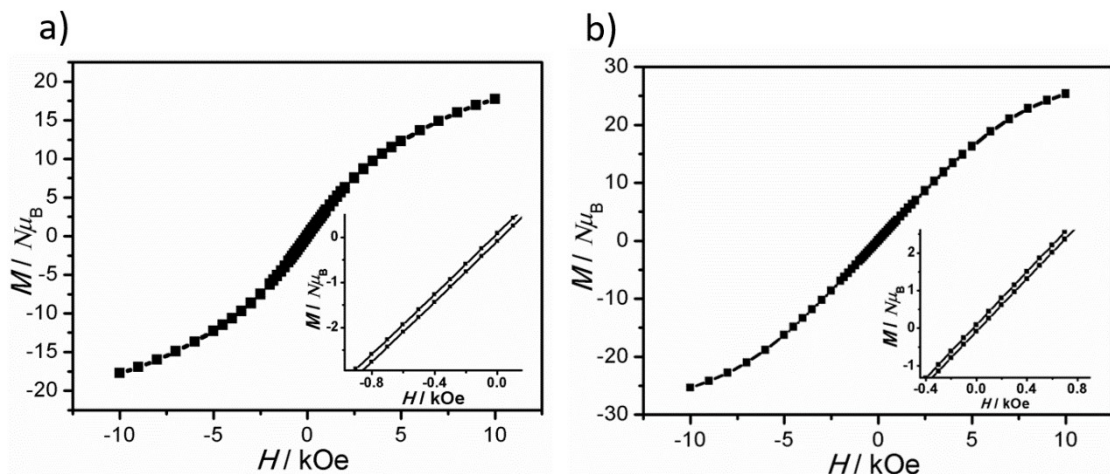


**Fig. S10** Plots of Magnetic hysteresis loops for **1** (a) and **2** (b).

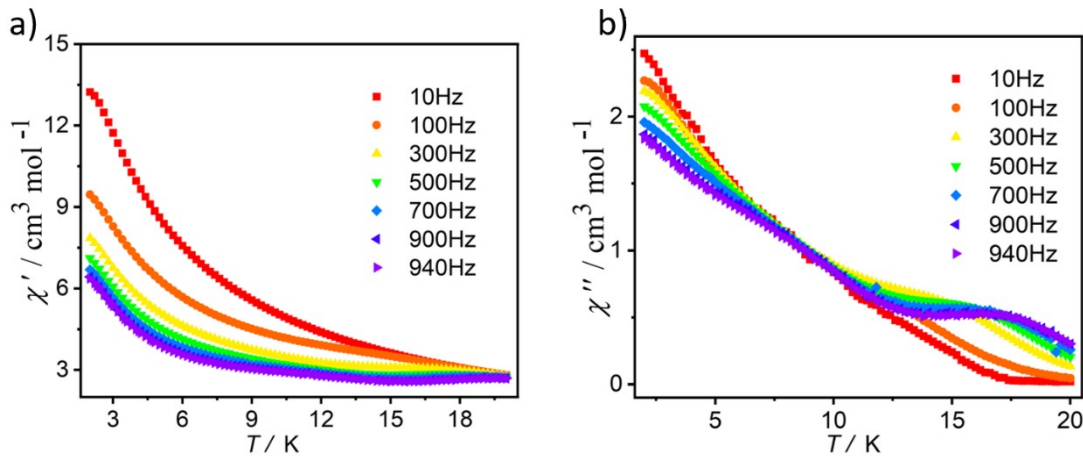


**Fig. S11** Temperature-dependent (a)  $\chi'$  and (b)  $\chi''$  ac susceptibilities under zero dc field for **1**.

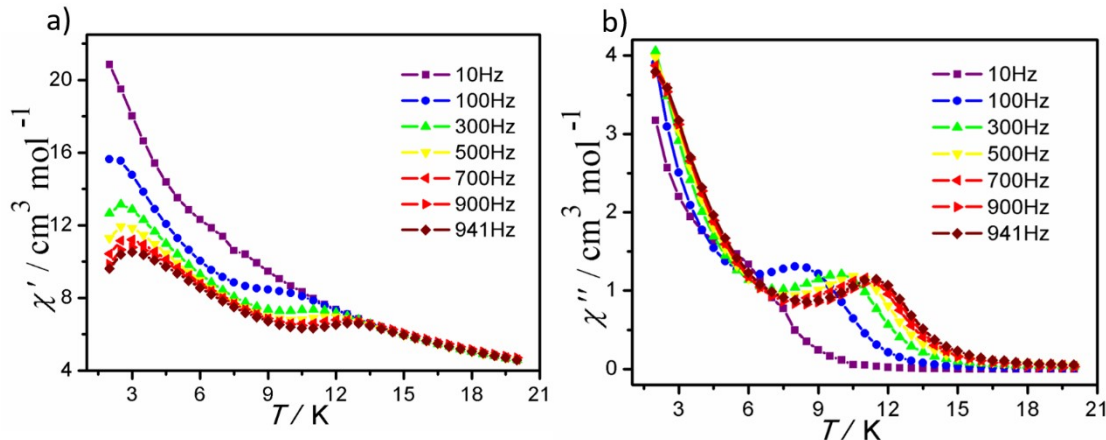


**Fig. S12** Temperature-dependent (a)  $\chi'$  and (b)  $\chi''$  ac susceptibilities under zero dc field for **2**.

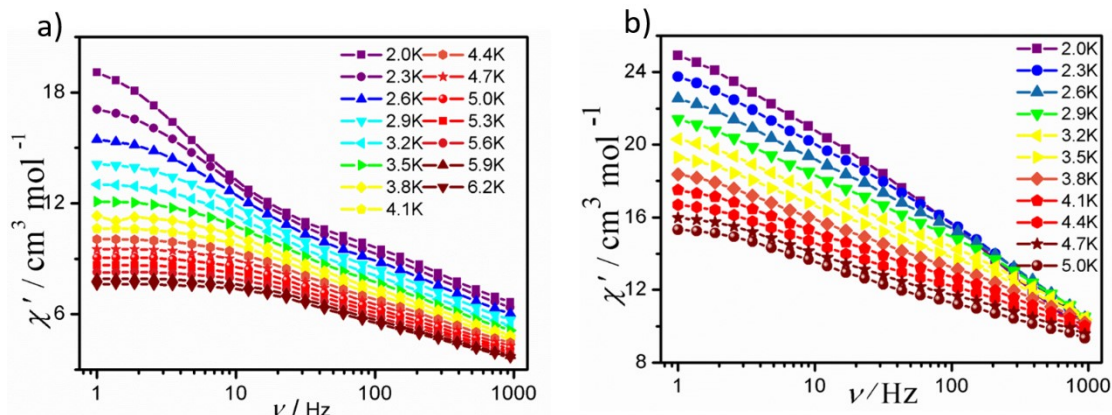


**Fig. S13** Plots of  $\chi'$  vs  $\nu$  (a) at 2.0-6.2 K and 2.0-5.0 K under a dc field of 0 Oe for **1** and **2**.

**Table S6.** Relaxation time ( $\tau$  / s) with the error for complex **1**.

1 (FR)		1 (SR)		
T	tau	tau_err	tau	tau_err
2.0	3.38462E-4	5.77126E-6	0.03278	8.21785E-4
2.3	3.36021E-4	6.56162E-6	0.02357	8.58735E-4
2.6	3.35801E-4	7.66749E-6	0.01815	8.61034E-4
2.9	3.29588E-4	8.28903E-6	0.01464	8.74872E-4
3.2	3.28574E-4	7.60533E-6	0.01217	8.60597E-4
3.5	3.22099E-4	7.66717E-6	0.01038	8.37678E-4
3.8	3.09327E-4	7.85395E-6	0.009	9.85016E-4
4.1	2.84613E-4	7.08028E-6	0.00798	7.9962E-4
4.4	2.72456E-4	7.02313E-6	0.0071	7.86438E-4
4.7	2.56648E-4	9.03056E-6	0.0064	7.60782E-4
5.0	2.37442E-4	8.79552E-6	0.0058	7.59708E-4
5.3	2.27402E-4	8.58745E-6	0.00532	7.40514E-4
5.6	2.13909E-4	7.34948E-6	0.00487	7.32866E-4
5.9	2.06923E-4	7.29622E-6	0.00448	7.28102E-4
6.2	1.92343E-4	7.35153E-6	0.00414	7.38579E-4

**Table S7.** Relaxation time ( $\tau$  / s) with the error for complex **2**.

2 (FR)		2 (SR)		
T	tau	tau_err	tau	tau_err
2.0	5.55525E-4	2.34323E-5	0.04459	0.00228
2.3	3.21269E-4	2.23459E-5	0.0436	0.00178
2.6	2.15459E-4	2.75539E-5	0.04149	0.00119
2.9	1.11379E-4	2.76643E-5	0.03644	0.0019
3.2	8.24647E-5	2.98877E-6	0.03359	0.00189
3.5	5.98953E-5	2.75657E-6	0.03009	0.00166
3.8	4.56117E-5	2.85016E-6	0.02776	0.00161
4.1	3.53631E-5	2.4545E-6	0.02466	0.00152
4.4	2.73197E-5	1.65646E-6	0.02165	0.00138
4.7	2.07832E-5	1.87586E-6	0.01868	0.00156
5.0	1.5922E-5	1.97755E-6	0.01595	0.00113

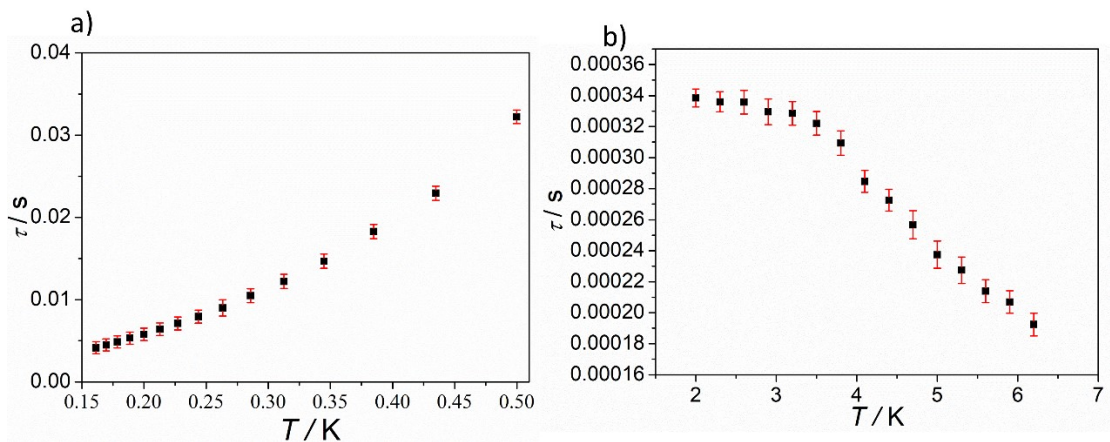


**Fig. S14** Plots of  $\tau$  vs  $T$  with the error for complexes **1**.

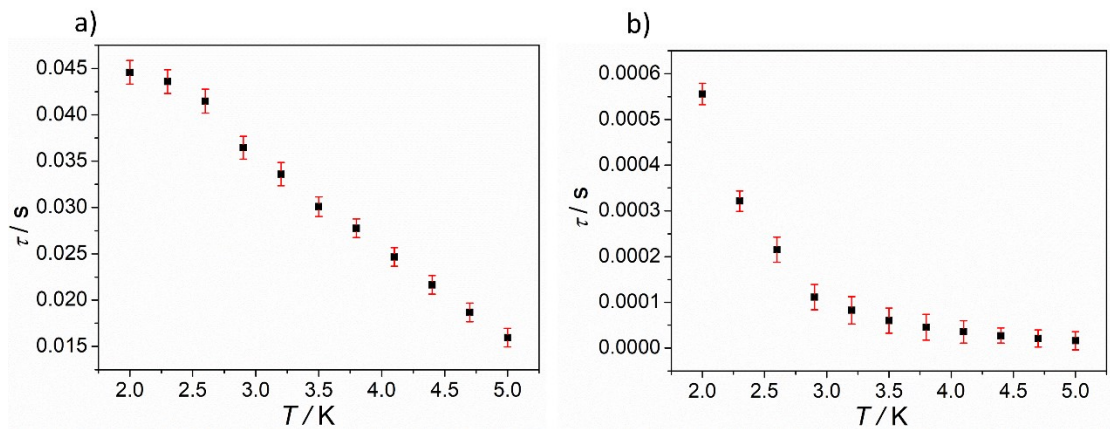


**Fig. S15** Plots of  $\tau$  vs  $T$  with the error for complexes **2**.

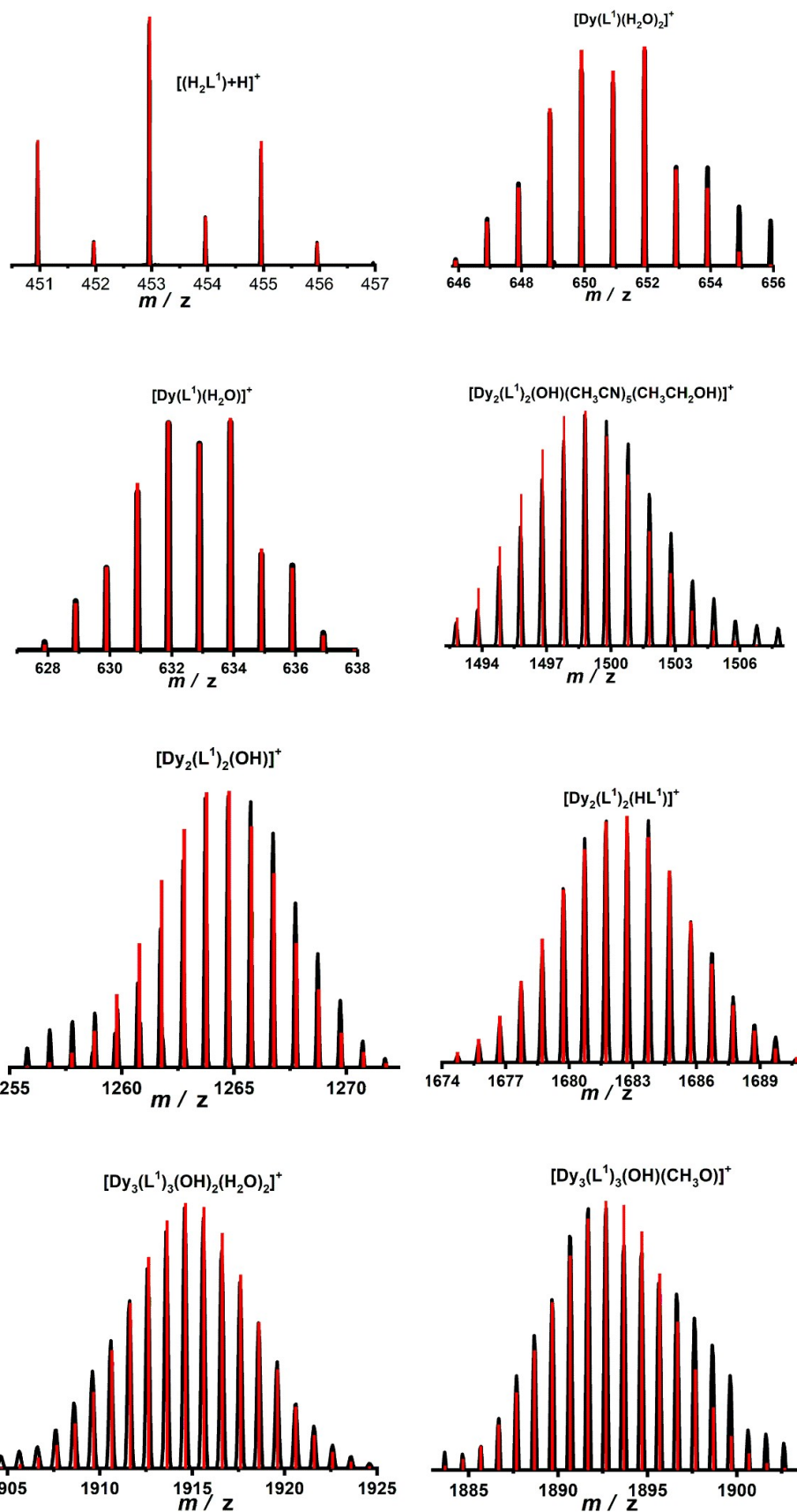


**Fig. S16.** The superposed simulated and observed spectra of several species for **1** (In-Source CID 0 eV).

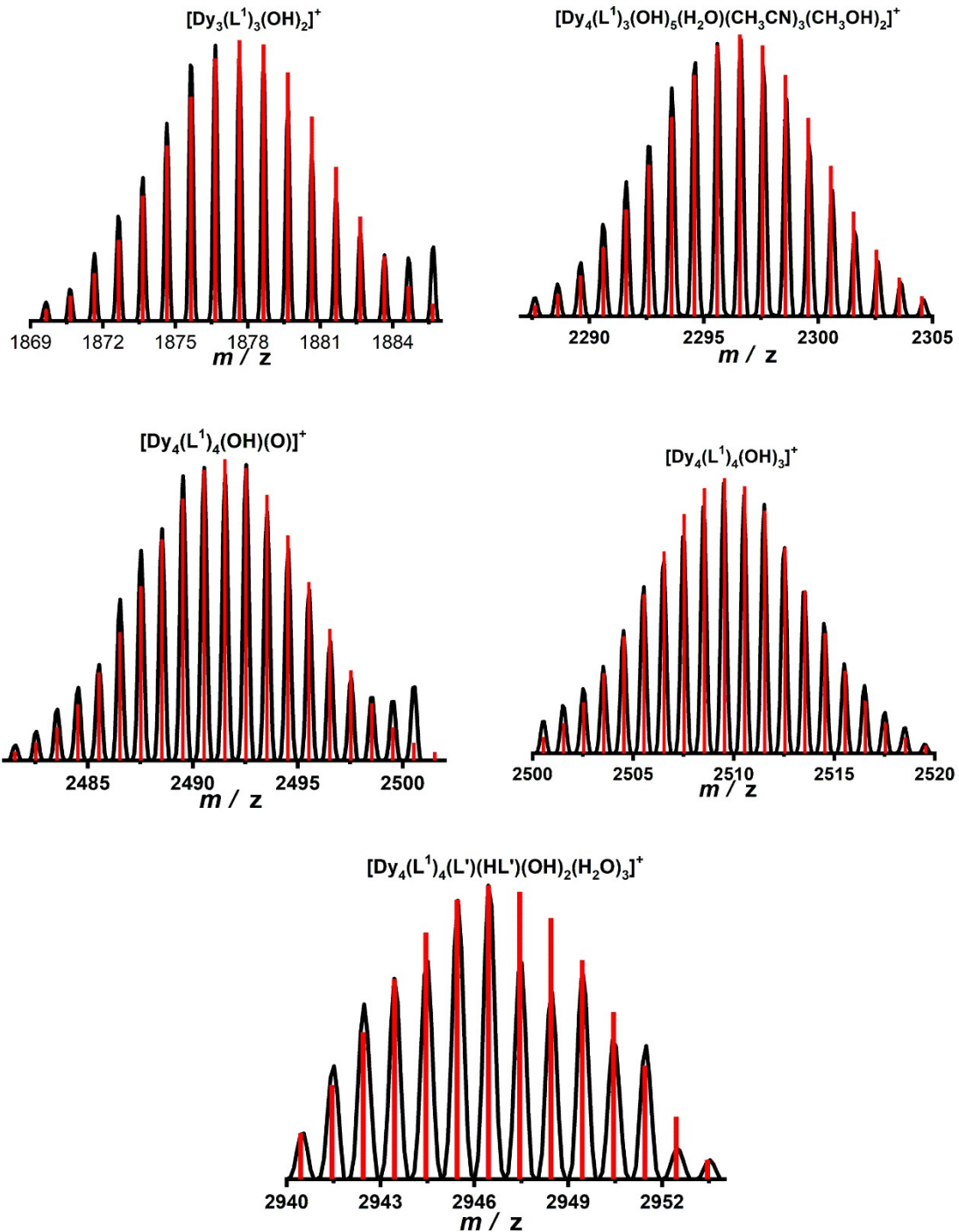


**Fig. S17.** The superposed simulated and observed spectra of several species for **1** (In-Source CID 0 eV).

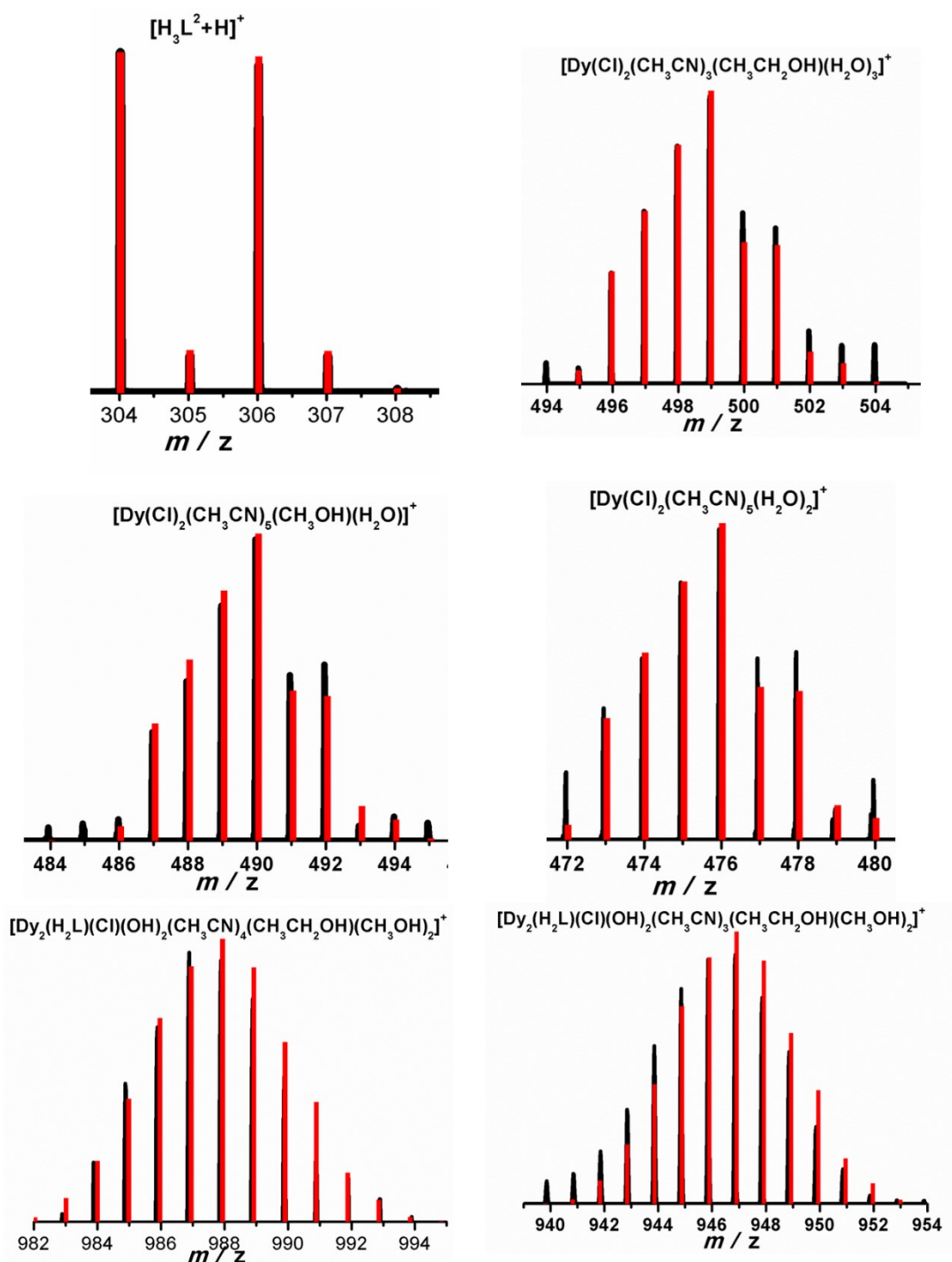


**Fig. S18.** The superposed simulated and observed spectra of several species for **2** (In-Source CID 0 eV).

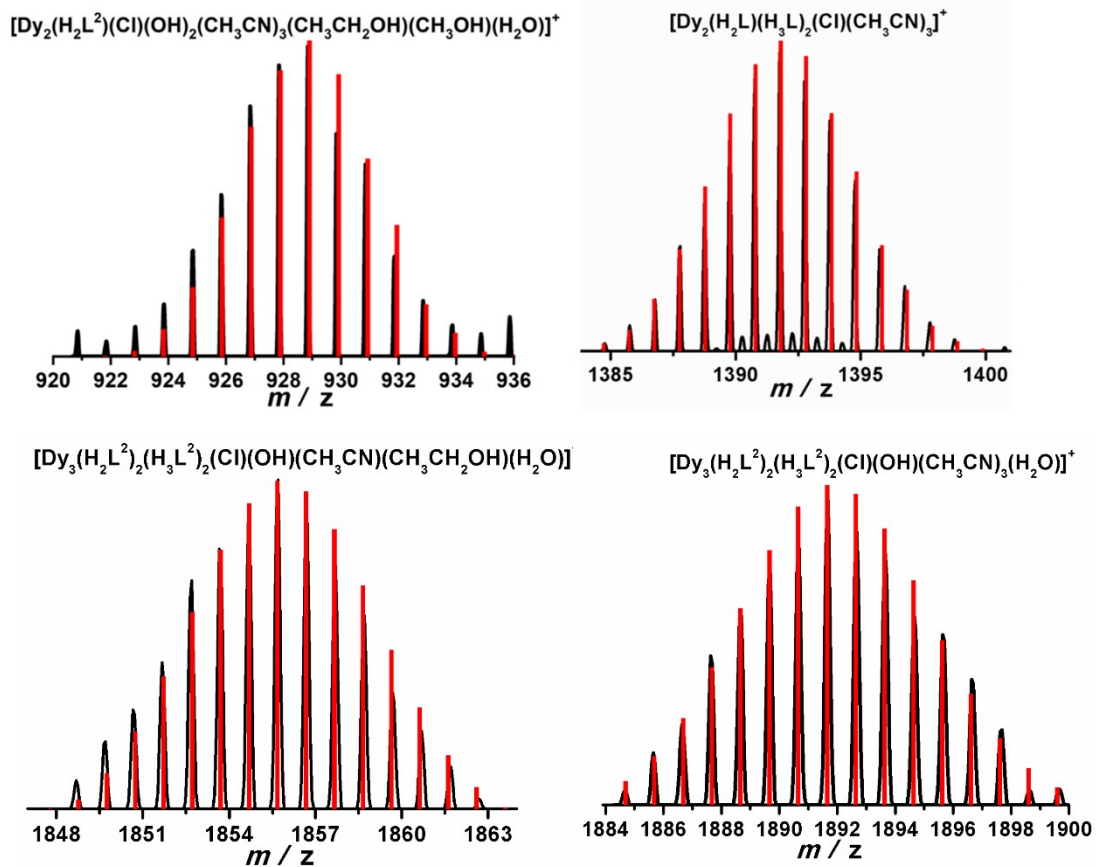


**Fig. S19.** The superposed simulated and observed spectra of several species for **2** (In-Source CID 0 eV).

**Table S8.** Major species assigned in the HRESI-MS of **1** in positive mode

Fragment	Relative Intensity									
	5 min	15 min	25 min	40 min	60 min	90 min	130 min	180 min	240 min	360 min
L <sup>1</sup>	0.90	0.12	0.05	0	0	0	0	0	0	0
DyL <sup>1</sup>	0.10	0.30	0.40	0.50	0.70	0.19	0.1	0	0	0
Dy <sub>2</sub> (L <sup>1</sup> ) <sub>2</sub>	0.05	0.20	0.30	0.40	0.50	0.70	0.60	0.50	0.40	0.10
Dy <sub>2</sub> (L <sup>1</sup> ) <sub>3</sub>	0.03	0.05	0.10	0.11	0.18	0.28	0.55	0.56	0.35	0.32
Dy <sub>3</sub> (L <sup>1</sup> ) <sub>3</sub>	0	0.15	0.20	0.30	0.71	0.72	0.85	0.75	0.62	0.54
Dy <sub>4</sub> (L <sup>1</sup> ) <sub>3</sub>	0	0.30	0.45	0.40	0.50	0.60	0.85	0.76	0.67	0.60
Dy <sub>4</sub> (L <sup>1</sup> ) <sub>4</sub>	0	0	0.08	0.14	0.20	0.22	0.31	0.48	0.65	0.51
Dy <sub>4</sub> (L <sup>1</sup> ) <sub>4</sub> (L') <sub>2</sub>	0	0	0	0	0	0	0.10	0.21	0.30	0.80

**Table S9.** Major species assigned in the HRESI-MS of **2** in positive mode

Fragment	Relative Intensity									
	5 min	10 min	20 min	40 min	60 min	120 min	240 min	360 min	480 min	600 min
L <sup>2</sup>	0.90	0.82	0.85	0.71	0.70	0.65	0.23	0.20	0.10	0.10
Dy	0.10	0.12	0.20	0.28	0.40	0.60	0.56	0.60	0.56	0.60
Dy <sub>2</sub> (L <sup>2</sup> )	0	0	0	0.06	0.11	0.14	0.56	0.50	0.52	0.35
Dy <sub>2</sub> (L <sup>2</sup> ) <sub>3</sub>	0	0	0	0	0.02	0.07	0.66	0.75	0.69	0.30
Dy <sub>3</sub> (L <sup>2</sup> ) <sub>4</sub>	0	0	0	0	0.02	0.06	0.13	0.58	0.55	0.54
Dy <sub>6</sub> (L <sup>2</sup> ) <sub>6</sub>	0	0	0	0	0	0	0.10	0.20	0.30	0.80